Physica A 390 (2011) 1033–1041

Contents lists available at ScienceDirect

Physica A

journal homepage: www.elsevier.com/locate/physa

Band structure and dynamic behaviors of Bose–Einstein condensates in Fourier-Synthesized optical lattices

Yan Chen [a,*], Li-Bin Fu [b], Yong Chen [a,c]

[a] Institute of Theoretical Physics, Lanzhou University, Lanzhou 730000, China

[b] Institute of Applied Physics and Computational Mathematics, Beijing 100088, China

[c] Key Laboratory for Magnetism and Magnetic Materials of the Ministry of Education, Lanzhou University, Lanzhou 730000, China

ARTICLE INFO

Article history:
Received 31 March 2010
Received in revised form 6 September 2010
Available online 8 December 2010

Keywords:
Band structure
Bose–Einstein condensates
Optical lattice

ABSTRACT

By employing a nonlinear three-mode model, we study the band structure of Bose–Einstein condensates in Fourier-Synthesized optical lattices, where the nonlinearity comes from the mean field treatment of interaction between atoms. In linear case, we present the band structure of the system. It is demonstrated that the energy band structure is strongly dependent on the value of relative phase of the two lattice harmonics. In the nonlinear case, we show that the eigenenergies as the functions of the quasi-momentum have a novel bowl structure in the middle energy level. It is found that there exist four critical values of interaction strength at which the band structure will undergo interesting changes. Furthermore, the stability of the eigenstate is also investigated.

1. Introduction

In recent years, Bose–Einstein condensates (BECs) in optical lattices have attracted enormous attention both experimentally and theoretically [1,2]. This is mainly because the lattice parameters and interaction strength can be manipulated by using modern experimental techniques. Researchers have discovered many novel phenomena, such as, nonlinear Landau–Zener tunneling, energetic and dynamical instability and the strongly inhibited transport of one-dimensional BEC in optical lattices [3–12]. One of the surprising discoveries is that the interaction between particles can influence the band structure dramatically [3,7].

Recently, ample interests have arisen in the field of transport properties of atoms and BECs subject to a Fourier-synthesized optical lattice (FS) [13,14]. The FS optical lattice is realized by superimposing a conventional standing wave potential of $\lambda/2$ spatial periodicity with a fourth-order multiphoton potential of $\lambda/4$ periodicity. The symmetric properties of such lattices can be controlled by the relative phase between the two standing waves, and the transport behaviors can be manipulated easily by the relative phase between the two spatial lattice harmonics. The transport properties of quantum objects subject to a periodic potential are determined by the band structure. So, the study of band structures for such FS optical lattices attracts many physicists. Here, we will focus on studying the band structure of BECs in a FS optical lattice.

In this paper, a nonlinear three-mode model is established based on the Gross–Pitaevskii (GP) equation with a FS optical lattice, where the nonlinearity comes from the mean field treatment of the interaction between condensate atoms. With this model, we reproduce the band structures of the lowest three levels for the linear case obtained in Ref. [13]. But in the nonlinear case, a more complicated band structure emerges with increasing interaction strength and a bowl structure is observed when the interaction exceeds a critical value. At the same time, several criteria are found in which the band structure will undergo interesting changes. In addition, the stabilities of the corresponding eigenstates are also studied.

* Corresponding author. Tel.: +86 13919086720.
E-mail addresses: chyanjp@gmail.com (Y. Chen), ychen@lzu.edu.cn (Y. Chen).

0378-4371/$ – see front matter © 2010 Elsevier B.V. All rights reserved.
doi:10.1016/j.physa.2010.11.045

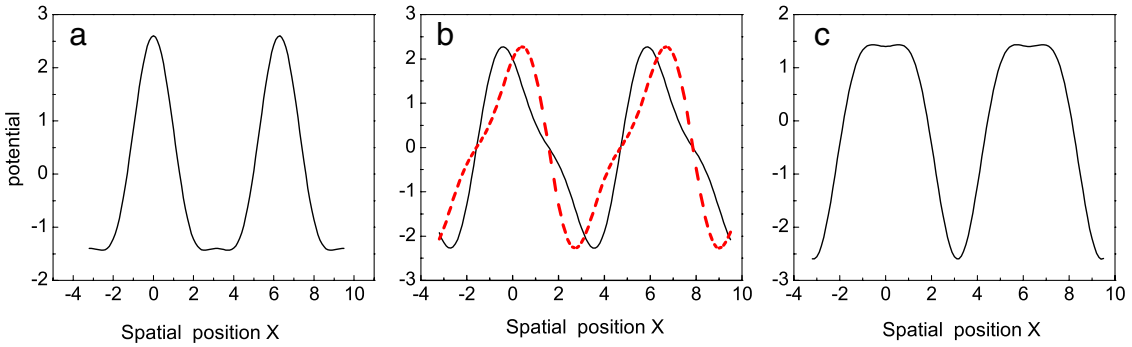

Fig. 1. Spatial potential for a periodic atom potential for different values of the phase α between lattice harmonics: (a) $\alpha = 0$, (b) $\alpha = \pi/2$ (solid line) and $\alpha = -\pi/2$ (dashed line), (c) $\alpha = \pi$. We have set $V_1 = 2$, $V_2 = 0.6$.

This paper is organized as follows. In Section 2, we obtain a dynamical equation describing the energy band properties of BEC in a FS optical lattice with three-mode approximation. In Section 3, the band structure of the periodic potential was derived by solving the eigenvalue equation of the system. There exists very particularly the energy band structure at the first Brillouin zone. Here, the main results and discussions are presented. In Section 4, we investigate the stability of the condensate by the Jacobian of the classical Hamiltonian. The summary and conclusion of our work are presented in Section 5.

2. Governing equations and three-mode approximations

We focus our attention on the situation that BEC is loaded into a one dimensional Fourier-synthesized optical lattices where the motion in perpendicular directions is confined. Here, the FS optical lattices are given by

$$V(x) = V_1 \cos(2k_0 x) + V_2 \cos(4k_0 x + \alpha) \tag{1}$$

where V_1 and V_2 denote the potential depths of two lattice harmonics respectively, k_0 is the wave number of the laser light which is used to generate the optical lattice, and α is the relative phase of two lattices. The shape and symmetry of the lattice depend on the relative phase of the two lattices, which is shown in Fig. 1. It is obvious that the lattice potential resembles a periodic sequence of hills for $\alpha = 0$ [Fig. 1(a)], the situation of spatial lattice potentials with the sawtooth-like structures are shown in Fig. 1(b) for $\alpha = \pm\pi/2$, and an array of potential dimples in the spatial lattice structure for $\alpha = \pi$ [Fig. 1(c)]. The values of the relative phase impact greatly on the band structure of the system which can be seen from the latter calculation. In the mean-field approximation, the dynamics of BEC can be modeled by the 1D-GP (Gross–Pitaevskii) equation in the comoving frame of the lattice,

$$\mathrm{i}\hbar\frac{\partial\psi}{\partial t} = -\frac{\hbar^2}{2m}\frac{\partial^2}{\partial x^2}\psi + V_1\cos(2k_0x)\psi + V_2\cos(4k_0x+\alpha)\psi + \frac{4\pi\,\hbar^2\,a_s}{m}|\psi|^2\psi \tag{2}$$

where ψ is the wave function of the condensate, m is the mass of atoms, a_s is the two-body s-wave scattering length, k_0 is the wave number of the laser light which is used to generate the optical lattice. The first Brillouin zone is $[-k_0, k_0]$. For convenience, we cast Eq. (2) into the dimensionless form

$$\mathrm{i}\frac{\partial\psi}{\partial t} = -\frac{1}{2}\frac{\partial^2}{\partial x^2}\psi + v_1\cos(x)\psi + v_2\cos(2x+\alpha)\psi + c|\psi|^2\psi. \tag{3}$$

The dimensionless variables are scaled as,

$$x \sim 2k_0x, \qquad \psi \sim \frac{\psi}{\sqrt{n_0}}, \qquad t \sim \frac{4\hbar}{m}k_0^2t,$$

where the variable are scaled as

$$v_i = \frac{mV_i}{4\,\hbar^2\,k_0^2}, \qquad c = \frac{\pi n_0 a_s}{k_0^2}.$$

Here, n_0 is the average density of the BEC, v_i represents the strength of the potential and c denotes the atomic interaction. In our following discussions, we focus on the case of repulsive interaction between atoms. i.e. $c > 0$.

We consider following three-state model to describe the band structure of the system

$$\psi = a_l(t)\mathrm{e}^{\mathrm{i}(k-1)x} + a_0(t)\mathrm{e}^{\mathrm{i}kx} + a_r(t)\mathrm{e}^{\mathrm{i}(k+1)x}$$

where the total probability $|a_l|^2 + |a_0|^2 + |a_r|^2 = 1$, $\hbar k$ is the quasi-momentum. As shown in Refs. [14,15], the three-mode approximation can give an exact solution to the GP equation at the first Brillouin and qualitatively reproduces the behavior

of the asymptotic time-averaged current. Further the three-mode approximation is valid for the lower energy state. We are interested in discussing the lower energy band near the first Brillouin zone. So the three-mode approximation should be a good approximation because of its clear physical meaning and trustworthyness [13]. Substituting this wave function into Eq. (3) and performing spatial integrals, we get

$$\mathrm{i}\frac{\mathrm{d}}{\mathrm{d}t}\begin{pmatrix} a_l \\ a_0 \\ a_r \end{pmatrix} = H\begin{pmatrix} a_l \\ a_0 \\ a_r \end{pmatrix}, \tag{4}$$

where

$$H_1 = \begin{pmatrix} \frac{(k-1)^2}{2} + c(2-|a_l|^2) & \frac{v_1}{2} + ca_0a_r^* & \frac{v_2}{2}\mathrm{e}^{-\mathrm{i}\alpha} \\ \frac{v_1}{2} + ca_ra_0^* & \frac{k^2}{2} + c(2-|a_0|^2) & \frac{v_1}{2} + ca_la_0^* \\ \frac{v_2}{2}\mathrm{e}^{\mathrm{i}\alpha} & \frac{v_1}{2} + ca_0a_l^* & \frac{(k+1)^2}{2} + c(2-|a_r|^2) \end{pmatrix}. \tag{5}$$

Here, we focus on the energy band properties at the Brillouin zone edge, i.e. $k = 1/2$, so after the linearization of the quadratic kinetic terms around $k = 1/2$ and dropping the constant energy of $\frac{k^2+1}{2} + 2c$, the Hamiltonian of Eq. (6) is

$$H_2 = \begin{pmatrix} -k - c|a_l|^2 & \frac{v_1}{2} + ca_0a_r^* & \frac{v_2}{2}\mathrm{e}^{-\mathrm{i}\alpha} \\ \frac{v_1}{2} + ca_ra_0^* & -\frac{1}{2} - c|a_0|^2 & \frac{v_1}{2} + ca_la_0^* \\ \frac{v_2}{2}\mathrm{e}^{\mathrm{i}\alpha} & \frac{v_1}{2} + ca_0a_l^* & k - c|a_r|^2 \end{pmatrix}. \tag{6}$$

The above Hamiltonian is distinct from that of the trimer train model [15–17] in which the off-diagonal term vanishes. Actually, the trimer train model is a period boundary condition whereas the above model is not. This leads to very different physics phenomena even in the linear case.

The dynamics of the above quantum system can be depicted by a classical Hamiltonian of the two-degree freedom [18]. Let us show that $s_1 = |a_l|^2, s_2 = |a_0|^2, s_3 = |a_r|^2, \theta_1 = \arg a_l - \arg a_0,\ \theta_2 = \arg a_r - \arg a_0, s_1 + s_2 + s_3 = 1$, we can get the classical Hamiltonian,

$$\begin{aligned} H = {} & \left(\frac{1}{2} - k\right)s_1 + \left(\frac{1}{2} + k\right)s_2 - \frac{1}{2} - \frac{c}{2}(s_1^2 + s_2^2 + s_3^2) + v_1\sqrt{s_1s_3}\cos\theta_1 \\ & + v_1\sqrt{s_2s_3}\cos\theta_2 + v_2\sqrt{s_1s_2}\cos(\theta_2 - \theta_1 - \alpha) + 2cs_3\sqrt{s_1s_2}\cos(\theta_1 + \theta_2). \end{aligned} \tag{7}$$

s_1, θ_1 and s_2, θ_2 are two pairs of canonically conjugate variables of the classical Hamiltonian system governed by the following differential equation:

$$\dot{s_1} = -\frac{\partial H}{\partial \theta_1} = v_1\sqrt{s_1(1-s_1-s_2)}\sin\theta_1 - v_2\sqrt{s_1s_2}\sin(\theta_2 - \theta_1 - \alpha) + 2c(1-s_1-s_2)\sqrt{s_1s_2}\sin(\theta_1 + \theta_2). \tag{8}$$

$$\dot{s_2} = -\frac{\partial H}{\partial \theta_2} = v_1\sqrt{s_2(1-s_1-s_2)}\sin\theta_2 + v_2\sqrt{s_1s_2}\sin(\theta_2 - \theta_1 - \alpha) + 2c(1-s_1-s_2)\sqrt{s_1s_2}\sin(\theta_1 + \theta_2). \tag{9}$$

$$\begin{aligned} \dot{\theta_1} = \frac{\partial H}{\partial s_1} = {} & \left(\frac{1}{2} - k\right) - c(2s_1 + s_2 - 1) + c\left(\frac{s_2 - 3s_1s_2 - s_2^2}{\sqrt{s_1s_2}}\right)\cos(\theta_1 + \theta_2) + v_1\cos\theta_1\left(\frac{1 - 2s_1 - s_2}{2\sqrt{s_1(1-s_1-s_2)}}\right) \\ & - v_1\cos\theta_2\left(\frac{s_2}{2\sqrt{s_1(1-s_1-s_2)}}\right) + \frac{v_2s_2}{2\sqrt{s_1s_2}}\cos(\theta_2 - \theta_1 - \alpha) \end{aligned} \tag{10}$$

$$\begin{aligned} \dot{\theta_2} = \frac{\partial H}{\partial s_2} = {} & \left(\frac{1}{2} + k\right) - c(2s_2 + s_1 - 1) + c\left(\frac{s_1 - 3s_1s_2 - s_1^2}{\sqrt{s_1s_2}}\right)\cos(\theta_1 + \theta_2) + v_1\cos\theta_2\left(\frac{1 - 2s_2 - s_1}{2\sqrt{s_2(1-s_1-s_2)}}\right) \\ & - v_1\cos\theta_1\left(\frac{s_1}{2\sqrt{s_1(1-s_1-s_2)}}\right) + \frac{v_2s_1}{2\sqrt{s_1s_2}}\cos(\theta_2 - \theta_1 - \alpha). \end{aligned} \tag{11}$$

3. The band structure

According to Bloch's theory, the band structure of the periodic potential is just derived by solving the eigenvalue equation. In the following, we will discuss the energy band structure of BECs in FS optical lattices. It is easy to find, for α and $-\alpha$, the eigenvalue is same when the eigenfunctions have relations $a_i \to a_i^*$ $(i = l, 0, r)$. Hence, we only consider the case for $0 \le \alpha \le \pi$ in the following content.

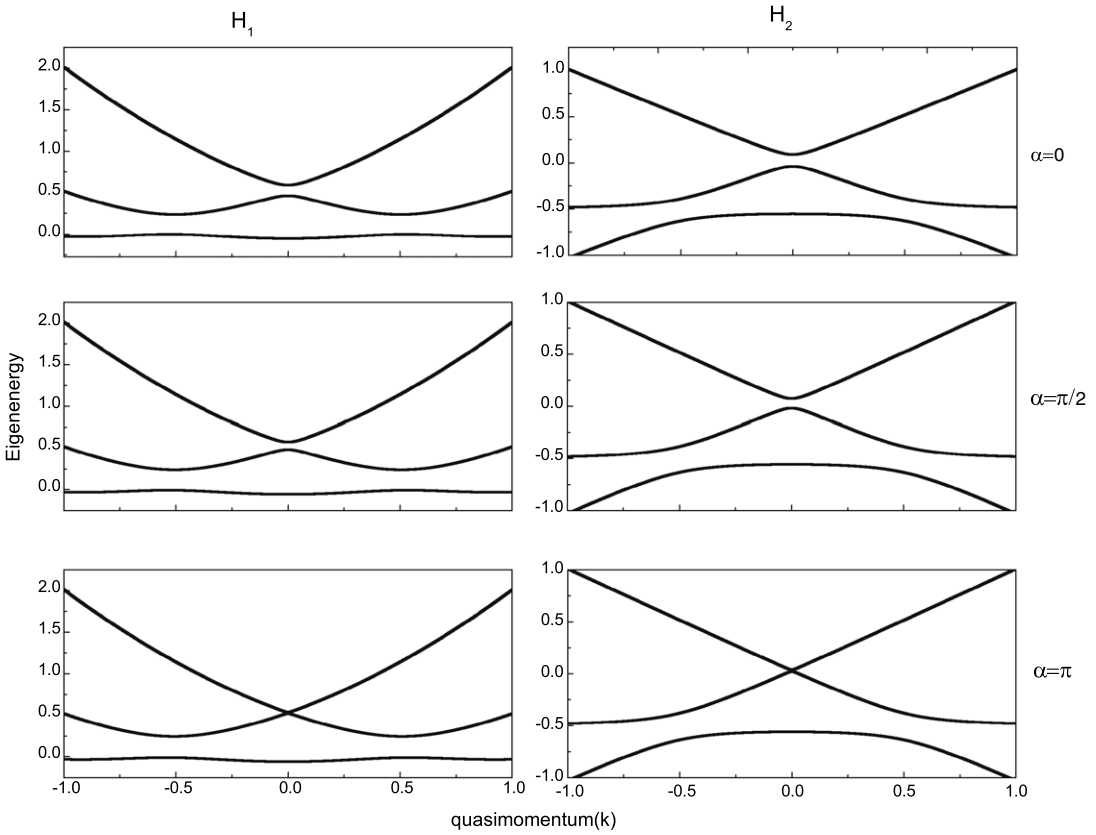

Fig. 2. Band structure of two spatial lattice harmonics in the linear case $c = 0$ for different phase. The first column denotes the eigenenergy of corresponding to Eq. (5), the second one is for Eq. (6) after dropping $\frac{k^2+1}{2} + 2c$. Here, we have set $\upsilon_1 = 0.25,\ \upsilon_2 = 0.075$.

3.1. Band structure of linear case

Fig. 2 shows the band structure of the spatial lattice harmonics in the linear case for differentα. The first column denotes the eigenenergy corresponding to Eq. (5) (H_1), the second column is for Eq. (6) (H_2) after dropping $\frac{k^2+1}{2} + 2c$. It is found that their levels are almost same, and the levels of the second column are shifted downward. So, in the following calculations, we only carried out the calculations with the Hamiltonian (H_2). It is clear that the gap between the first and second excited band is strongly dependent on the value of relative phase, and the band gap is determined by an analytical expression $\left|\frac{\upsilon_1^2}{8} + e^{i\alpha}\upsilon_2\right|$ which shows the two interfering contributions of the coupling Rabi frequencies arising from different lattice harmonics [13]. Our results are consistent with Ref. [13], and the only difference is potential value. Therefore, it is clear that the mean-field three-mode model is reliable for calculation of the band structure.

3.2. The band structure in the nonlinear case with $\alpha = 0$

The fixed point or the minimal energy point of the classical Hamiltonian system corresponds to the eigenstate of the quantum system [5,19]. Deducing the analytical expression of these fixed points is difficult. However, numerically, we can readily obtain them with the fourth-order Runge–Kutta method by setting $\dot{s_1} = \dot{s_2} = \dot{\theta_1} = \dot{\theta_2} = 0$ in the Eqs. (8)–(11). We plot the eigenenergies as the function of the quasi-momentum in Fig. 3 for $\alpha = 0$. They show an unusual loop structure with increasing interaction. For a very weak interaction, the eigenenergy levels are similar to the linear case ($c = 0$). With increasing nonlinearity (i.e., $c = 0.25$), the topological structure of the middle level (E_2) changes: a small loop emerges. When the interaction is stronger (i.e., $c = 0.75$), a new concave line emerges in the middle level E_2 and the topological structure of the lowest level E_3 changes: two small loops appear. Additionally when $c = 1$, a new convex line in Fig. 3(d) appears in E_2 and the two loops of the E_3 become large. When the interaction is stronger ($c = 1.25$), the new concave line, the new convex line and the loop of the middle level form a bowl structure. And two loops of the lowest level start to collide. With further increase of interaction ($c = 1.5$), the bowl structure runs into the band edge and the two loops of E_3 entangle each other. However, we can still distinguish these levels by their different phases. In fact, level E_1 has phases ($\theta_1 = 0, \theta_2 = 0$), level E_2 has phase ($\theta_1 = \pi, \theta_2 = \pi$), and level labeled by E_3 has phase ($\theta_1 = \pi, \theta_2 = 0$) or ($\theta_1 = 0, \theta_2 = \pi$). This interesting structure in a nonlinear system is very different from the behaviors of a linear system. Bloch waves at the Brillouin zone

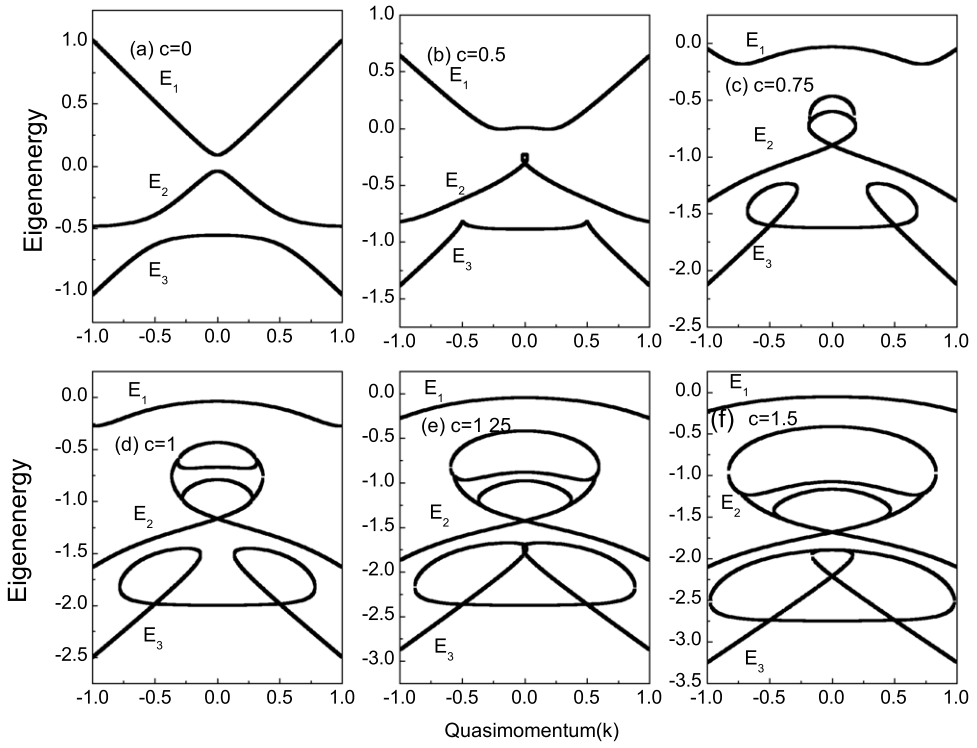

Fig. 3. The eigenenergy levels for different interaction strengths with fixed relative phase ($\alpha = 0$). We set $\upsilon_1 = 0.25,\ \upsilon_2 = 0.075$.

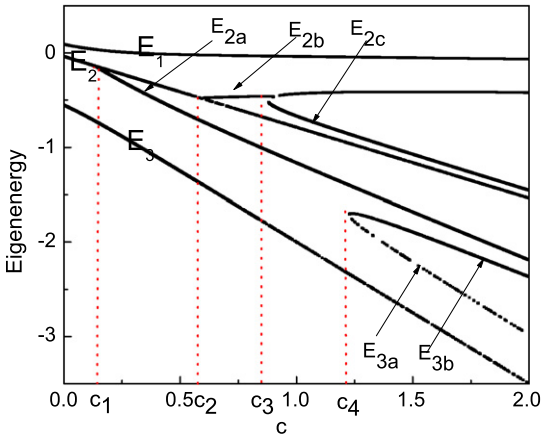

Fig. 4. When $k = 0$, the energy levels vary with the interaction strength c. Here, we set $\upsilon_1 = 0.25,\ \upsilon_2 = 0.075, \alpha = 0$.

edge always have zero velocity in a linear system, but in a nonlinear system it carries a nonzero velocity, as shown in Fig. 3. The nonzero velocity carried by these waves is a manifestation of the superfluidity of BECs. For free particles, the flow e^{ikx} is stopped completely by Bragg scattering; For the BECs, the flow is no longer stopped when the superfluidity is strong. So, the novel band structures emerges.

The relation between the chemical potential and the above energy is

$$E = \mu - \frac{c}{2}(|a_l|^4 + |a_0|^4 + |a_r|^4) \tag{12}$$

where μ signifies the chemical potential defined as $\langle\psi|H|\psi\rangle$.

From the above analysis, there exists a very interesting structure of the energy band in the position ($k = 0$) when we fix the relative phase. The dependence of the energy levels on the interaction strength is exposed by Fig. 4. When the interaction strength is less than a critical value $c_1 = 0.15$, the level structure is similar to its linear counterpart. For $c > c_1$, one level marked as E_{2a} emerges. Actually, it corresponds to the loop structure of E_2 in Fig. 3(b) ($c = 0.5$). When the interaction strength exceeds the second critical value $c_2 = 0.6$, the energy level labeled by E_{2b} emerges. It corresponds to the new

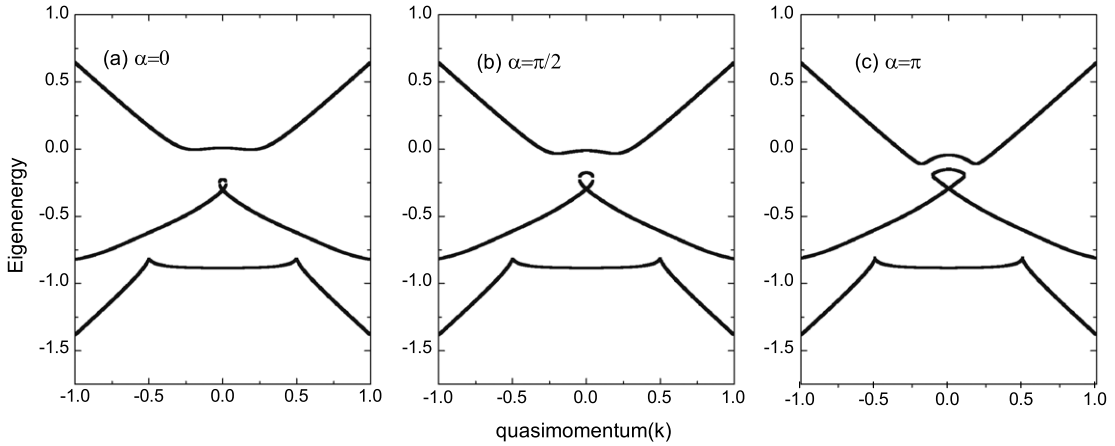

Fig. 5. Band structure of two spatial lattice harmonics in the nonlinear case (the weak interaction) $c = 0.25$ for different phases α. We have set $\upsilon_1 = 0.25,\ \upsilon_2 = 0.075$.

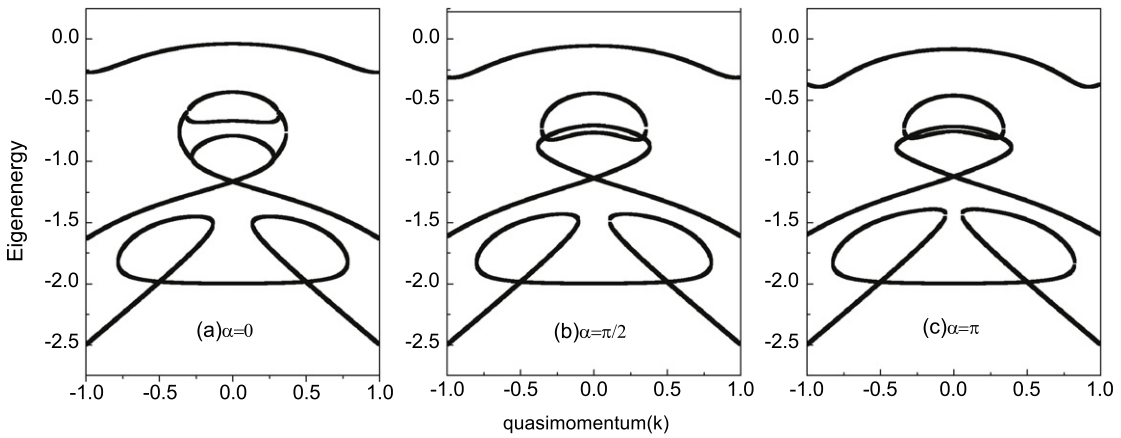

Fig. 6. Band structure of two spatial lattice harmonics in the nonlinear case (the strong interaction) $c = 1$ for different phases α. We have set $\upsilon_1 = 0.25,\ \upsilon_2 = 0.075$.

concave line of E_2 in Fig. 3(c) ($c = 0.75$). When the interaction strength exceeds the third critical value $c_3 = 0.88$, one level marked as E_{2c} appears. It corresponds to the new convex line of E_2 in Fig. 3(d) ($c = 1$) and has the same phases as that of E_2. For the weak interaction, the state adiabatically follows the curve in Fig. 3(a). However, in the case of strong interaction, the adiabatic condition is violated, the atoms of lower energy band tunnel slowly to higher bands. At the moment, the tunneling leads to the redistribution of the population located in each band. Thus, the energy curves terminate at some points in Fig. 3(d), where one has a crossing of local minima. One minimum corresponds to the fluid moving to the right, the other moving to the left. So the point of the higher energy branches is a local energy minimum of the system. From Ref. [20], when the Bloch waves are energy minima of system, they represent superflow, when the Bloch wave are energy saddle points they suffer Landau instability. So the point of the higher energy branches (E_{2b}, E_{2c}) is a local energy minimum and it is a superflow. When the interaction strength exceeds the fourth critical value $c_4 = 1.23$, two more energy levels labeled as (E_{3a}, E_{3b}) emerge. They correspond to the loop structures of mutual entanglement in the lower level E_3 and have the same phases as those of E_3.

3.3. Impacting of the relative phase on the band structure in the nonlinear case

We know that the band gap is strongly dependent on the value of the relative phase in the linear case, whereas, the value of the relative phase has a great impact on the band structure in the nonlinear case.

Fig. 5 shows the band structure for different relative phase α between lattice harmonics in the nonlinear case for the weak interaction. It is clear that the size of band gap between the first and second excited band decreases gradually when the relative phase varies from 0 to π, and the width of the loop increases. The eigenvalue is the same when the eigenfunctions have relations $a_i \to a_i^*$ ($i = l, 0, r$) for α and $-\alpha$. It means that the size of the band gap and the width of the loop undergo a period changing with varying of the relative phase. Similarly, for the stronger interaction, they have an analogous situation which is plotted in Fig. 6. In addition, the cross of the middle level has been opened when $\alpha = \pi$.

According to above analysis, we know that the change of the band structure is a manifestation of superfluidity, a phenomenon that manifests itself in many related ways, including dissipationless flow, quantized vortices, reductions in the moment of inertia, and the existence of persistent currents. A detailed discussion of this topic is given by Mueller [8]. For interacting systems in FS optical lattices, it is found that there are four different critical values of interaction strength where the complex loop structures appear. For strongly interacting condensate, the middle bands of FS optical lattices can look quite different than those of a sinusoidal lattice [21]. After the initial critical value of interaction strength is reached, a loop starts to form, as shown in Fig. 3(b). When the interaction strength increases, other critical values are reached where the width of the loop runs into the band edge. Eventually, the wave number that should be less than zero becomes imaginary due to the form of the potential. This represents a nonphysical solution and is contrary to the assumption that the phase is real. Therefore, the band appears as the nesting of two loops. These are shown in the middle energy of Fig. 3(e).

4. The stability of the Bloch states

The stability of Bloch states can be obtained by imposing a small perturbation on the stationary state, and to understand how it evolves with time. The system is unstable if the small deviation gains exponentially. It is stable if it just oscillates around the stationary state. To describe this phenomena quantitatively, we write down the wave function in the form $\psi = \psi_0 + \delta\psi$ and substitute it into the time-dependent Schrodinger equation

$$\mathrm{i}\frac{\partial\psi}{\partial t} = \left[-\frac{1}{2}\frac{\partial^2}{\partial x^2} + V(x) + c|\psi|^2\right]\psi. \tag{13}$$

The equation of $\delta\psi$ can be easily obtained after neglecting high order terms greater than 2.

$$\mathrm{i}\frac{\partial}{\partial t}\delta\psi = L\delta\psi + c\psi_0^2\delta\psi^*. \tag{14}$$

Here, $L = -\frac{1}{2}\frac{\partial^2}{\partial x^2} + V(x) + 2c|\psi_0|^2 - \mu$, ψ_0 is the stationary state and μ is corresponding chemical potential. The conjugate expression of the above equation reads,

$$\mathrm{i}\frac{\partial}{\partial t}\delta\psi^* = -L\delta\psi^* - c\psi_0^{*2}\delta\psi. \tag{15}$$

Rewrite them into a matrix form,

$$\mathrm{i}\frac{\partial}{\partial t}\begin{pmatrix}\delta\psi\\ \delta\psi^*\end{pmatrix} = \begin{pmatrix}L & c\psi_0^2\\ -c\psi_0^{*2} & -L\end{pmatrix}\begin{pmatrix}\delta\psi\\ \delta\psi^*\end{pmatrix}. \tag{16}$$

Since we are interested in a periodic system, ψ_0 is actually the Bloch states ψ_k, and the perturbation can be composed with $\mathrm{e}^{\mathrm{i}kx}[u(x,t)\mathrm{e}^{\mathrm{i}qx} + v^*(x,t)\mathrm{e}^{-\mathrm{i}qx}]$. Substituting them into above equation yields

$$\mathrm{i}\frac{\partial}{\partial t}\begin{pmatrix}u\\ v\end{pmatrix} = \begin{pmatrix}L(k+q) & c\psi_k^2\\ -c\psi_k^{*2} & -L(-k+q)\end{pmatrix}\begin{pmatrix}u\\ v\end{pmatrix}. \tag{17}$$

For numerical calculations, one still need to expand $u(x,t)$ and $v(x,t)$ into a Fourier series. The stability of BEC in a cos-*potential* has been extensively studied in Ref. [3].

$$H_J = \begin{pmatrix}-\frac{\partial^2 H}{\partial s_1\partial\theta_1} & -\frac{\partial^2 H}{\partial\theta_1^2} & -\frac{\partial^2 H}{\partial s_3\partial\theta_1} & -\frac{\partial^2 H}{\partial\theta_3\partial\theta_1}\\ \frac{\partial^2 H}{\partial s_1^2} & \frac{\partial^2 H}{\partial\theta_1\partial s_1} & \frac{\partial^2 H}{\partial s_3\partial s_1} & \frac{\partial^2 H}{\partial\theta_3\partial s_1}\\ -\frac{\partial^2 H}{\partial s_1\partial\theta_3} & -\frac{\partial^2 H}{\partial\theta_1\partial\theta_3} & -\frac{\partial^2 H}{\partial s_3\partial\theta_3} & -\frac{\partial^2 H}{\partial\theta_3^2}\\ \frac{\partial^2 H}{\partial s_1\partial s_3} & \frac{\partial^2 H}{\partial\theta_1\partial s_3} & \frac{\partial^2 H}{\partial s_3^2} & \frac{\partial^2 H}{\partial\theta_3\partial s_3}\end{pmatrix}. \tag{18}$$

Here, we mainly present the stabilities at $k = 0$ and $k = 1/2$ which are related to the lowest energy band and the middle energy band in the FS optical system. The stability of the corresponding eigenstates can be evaluated by the eigenvalues of the Jacobian H_J. The eigenvalues of the Jacobian have their correspondence of the Bogoliubov excitation spectrum of BECs. A real value indicates a stable BEC state, whereas the emergence of an imaginary value implies instability for BECs and leads to a rapid production of the Bogoliubov quasi-particles in Ref. [4,22]. According to the above analysis, the adiabatic condition is violated for the strong interaction. Where the system strays away from original eigenstate, it leads to a tunnel between different eigenstates. This adiabatic condition can also be specified in terms of the Bogoliubiv spectrum. If the Bogliubov

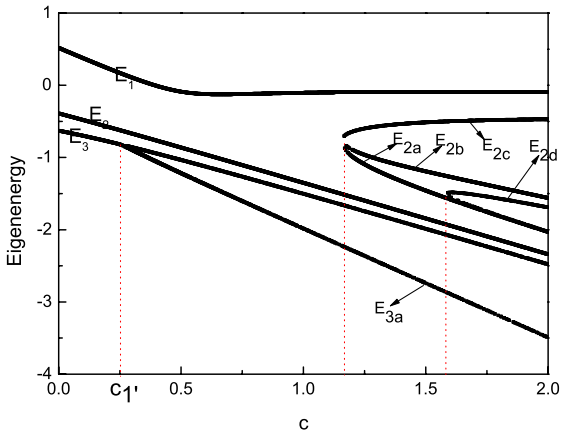

Fig. 7. When $k = 1/2$, the energy levels vary with the interaction strength c, we have set $\upsilon_1 = 0.25,\ \upsilon_2 = 0.075, \alpha = 0$.

spectrum is real, the adiabaticity is kept; otherwise, it is broken [20]. By calculating the Jacobian matrix and making the diagonalization, we know the states corresponding to levels E_{2b}, E_{2c} and E_{3b} are unstable. It means that the Bogliubov spectrum corresponding to levels E_{2b}, E_{2c} are imaginary, the adiabaticity is broken. Thus the point of the higher energy branches (E_{2b}, E_{2c}) is a local energy minimum, and the branch is unstable. Similarly, energy branches corresponding to (E_{2a}, E_{2b}) and (E_{3a}, E_{3b}) are also unstable. Additionally, the stability at $k = 1/2$ is shown in Fig. 7. Its analysis and explanation are similar to those of stability at $k = 1/2$. Therein, levels E_{2a} and E_{3a} are stable, others are unstable states. By comparing the stability at $k = 0$ with the stability at $k = 1/2$, we found that the critical value of the appearing loop structure increases ($c_1 = 0.15$ at $k = 0$, while $c_1' = 0.25$ at $k = 1/2$) with the increasing k value, while their stability results are consistent each other.

5. Summary and discussion

To summarize, we have investigated the properties of BECs in FS optical lattices in the nonlinear case. We describe the band structure in a FS atom potential realized by superimposing two lattice potentials of spatial periodicities $\lambda/2$ and $\lambda/4$, $V(x) = V_1 \cos(2k_0 x) + V_2 \cos(4k_0 x + \alpha)$. The spatial lattice potential for different values of the relative phase has different shapes. In this premise, with the mean-field theory and three-mode approximation, we obtain a dimensionless Schrödinger equation describing the properties of BECs in FS optical lattices. By solving the eigenvalue equation of the Hamiltonian (Eq. (5)) we get the band structure for different values of the relative phase α of the two spatial lattice harmonics in the linear case, which are consistent with the results in Ref. [13]. And, there exists a very novel band structure with a fixed relative phase in the nonlinear case. A bowl structure emerges when $c > 0.88$. At the same time, it is found that there exist four critical values ($c_1 = 0.25,\ c_2 = 0.6,\ c_3 = 0.88,\ c_4 = 1.23$) in which the band structure undergoes interesting changes. Besides, changing of the relative phase impacts greatly on the properties of the energy structure when the interaction strength is set. Perhaps the change of the band structure produces the behavior of the asymptotic time-averaged current. Furthermore, we analyze the stability of the corresponding eigenstates by the eigenvalues of the Jacobian of the classical Hamiltonian. We hope our theoretical discussion will stimulate experiments in this direction.

Acknowledgements

This work was supported by the National Natural Science Foundation of China under Grant No. 10975063 and by the Open Project of Key Laboratory for Magnetism and Magnetic Materials of the Ministry of Education, Lanzhou University. We are grateful to J.K. Xue for help discussions.

References

[1] O. Morsch, M. Oberthaler, Rev. Modern Phys. 78 (2006) 179.
[2] I. Bloch, J. Dalibard, W. Zwerger, Rev. Modern Phys. 80 (2008) 885.
[3] B. Wu, Q. Niu, Phys. Rev. A 61 (2000) 023402;
B. Wu, Q. Niu, Phys. Rev. A 64 (2001) 061603;
B. Wu, R.B. Diener, Q. Niu, Phys. Rev. A 65 (2002) 025601.
[4] Z.P. Karkuszewski, K. Sacha, A. Smerzi, Eur. Phys. J. D 21 (2002) 251.
[5] J. Liu, et al., Phys. Rev. A 66 (2002) 023404.
[6] M. Jona-Lsinio, O. Morsh, M. Cristiani, N. Malossi, J.H. Muller, E. Couritade, M. Anderlini, E. Arumondo, Phys. Rev. Lett. 91 (2003) 230406.
[7] D. Diakonov, et al., Phys. Rev. A 66 (2002) 013064.
[8] E.J. Mueller, Phys. Rev. A 66 (2002) 063603.
[9] L. Fallni, L.D. Sarlo, J.E. Lye, M. Modugno, R. Saer, C. Fort, M. Inguscio, Phys. Rev. Lett. 93 (2004) 140406.

[10] T. Koponen, J.P. Martikainen, J. Kinnunen, P. Törmä, Phys. Rev. A 73 (2006) 033620.
[11] B. Liu, L.B. Fu, S.P. Yang, J. Liu, Phys. Rev. A 75 (2007) 033601;
L.B. Fu, J. Liu, Phys. Rev. A 74 (2006) 063614.
[12] J.C. Bronski, et al., Phys. Rev. Lett. 86 (2001) 1402;
J.C. Bronski, et al., Phys. Rev. E 63 (2001) 036612.
[13] T. Salger, C. Geckeler, S. Kling, M. Weitz, Phys. Rev. Lett. 99 (2007) 190405.
[14] D. Poletti, G. Benenti, G. Casati, B.W. Li, Phys. Rev. Lett. 102 (2009) 130604.
[15] R. Franzosi, V. Penna, Phys. Rev. A 63 (2001) 013601.
[16] R. Franzosi, V. Penna, Phys. Rev. E 67 (2003) 046227.
[17] P. Buonsante, R. Franzosi, V. Penna, Phys. Rev. Lett. 90 (2003) 050404.
[18] E.M. Graefe, H.J. Korsch, D. Witthaut, Phys. Rev. A 73 (2006) 013617.
[19] J. Liu, B. Wu, Q. Niu, Phys. Rev. Lett. 90 (2003) 170404.
[20] B. Wu, Q. Niu, New J. Phys. 5 (2003) 104.
[21] M. Machholm, C.J. Pethick, H. Smith, Phys. Rev. A 67 (2003) 053613.
[22] J. Liu, C.W. Zhang, Phys. Rev. A 73 (2006) 013601.